Supplementary materials

Supplementary Fig. 1 Model of direct PPARγ action in skeletal muscle, *in vivo*. **A-C** PPAR mRNA (**A**), protein (**B**), and activity (**C**): Tibialis anterior of C57Bl/6J mice was injected with 15 μg pSV-PPARγ1 on one side, 15 μg pCMV-βgal on the contralateral side, and 5 μg pRL-TK plus 5 μg pPPREx3-LUC on both sides. PPAR activity was calculated as the ratio of firefly to Renilla luciferase activities, measured one week after transfection (* $p<0.05$, n=6; *** $p<0.00005$, n=8). The PPARγ protein content of brown adipose tissue (BAT) is shown for comparison. **D** Frozen sections from tibialis anterior transfected with 10 μg pCMV-βgal + 15 μg PPARγ on one side or 25 μg β-gal (contralateral side). Top panels: X-gal staining. Lower panels: AdipoRed staining.

Supplementary Fig. 2 Model of direct PPARγ action in skeletal myotubes. **A-C** In C2C12 myotubes, PPARγ mRNA (**A**), protein (**B**), and activity (**C**) were assessed 2 days after adenotransfection and 1 day after 500 nM rosiglitazone (Rosi) treatment. * $p<0.05$ versus adGFP transfected groups, ** $p<0.01$ versus all other experimental groups, n=3-4 per group. **D** PPARγ-activating ligand levels were assessed by measurement of secreted alkaline phosphatase (SEAP) accumulation in the media of myotubes transfected with a PPARγ ligand binding domain (LBD) based reporter construct. Myoblasts had been transfected with pFA-PPARγ-LBD and pFR-SEAP (see Supplementary Methods). # $p<0.0001$ versus vehicle treated cells. **E** Myotube morphology assessed by phase-contrast microscopy using a 10x objective; white bars represent 200 μm. Undifferentiated C2C12 myoblasts are shown for comparison. **F** Transcriptional markers of myocellular differentiation, myogenin (Myog) and myosin heavy chain 1 (Myh1), in C2C12 myotubes treated as indicated, with 3T3L1 fibroblasts and C2C12 myoblasts serving for comparison. Not detected, N.D. **G** Expression of other transcriptional markers. Cysteine-rich secretory protein 1 (CRISP1) is an adipose-selective gene which is not responsive to thiazolidinediones. Ancient ubiquitous protein 1 (AUP1) is a gene highly regulated by thiazolidinediones in mature adipocytes but with similar expression between muscle and adipose tissue. See Supplementary Methods for methods by which these markers were selected. In contrast to myoblast models of PPARγ action (Supplemental References 1-3), transdifferentiation to adipocytes is not observed in our models, presumably avoided by transfecting PPARγ into differentiated myocytes.

Supplementary Fig. 3 **A** AdipoRed (green) staining of neutral lipid droplets in myotubes cultured with media containing no added fatty acid (top panels) or 0.75 mM oleate + 0.3 mM albumin (bottom panels). Nuclei are stained blue with DAPI. **B** PPARγ overexpression increases myocellular triglyceride levels only when the media is supplemented with fatty acid. Total triglyceride levels were measured in myotubes incubated for 18 h with media with no added fatty acid (left group) or 0.75 mM oleate + 0.3 mM albumin (right group). C2C12 myotubes were treated with adGFP + vehicle (white bars), adGFP + 500 nM rosiglitazone (hatched), adPPARγ + vehicle (grey), or adPPARγ + 500 nM rosiglitazone (black). n=3, * $p<0.05$ versus adGFP, # $p<0.05$ versus adGFP + rosiglitazone. **C** Oxidation by myotubes of 80 μM [1-^{14}C]oleate complexed with 40 μM albumin over 2 h to acid soluble metabolites (partial oxidation, black bars, left axis) and $^{14}CO_2$ (grey bars, right axis). +DNP cells were pre-incubated with 200 μM 2,4-dinitrophenol (DNP) for 30 minutes prior to measurement of oxidation.

Supplementary Fig. 4 Rosiglitazone dose response for insulin-stimulated AKT phosphorylation. **A** Myotubes were treated with rosiglitazone for 24 h, then 10 nM insulin for 10 min. Grey lines represent non-linear fits for EC_{50}=5 nM. Top panel: adGFP transfected cells, n=2-5 per point. Bottom panel: adPPARγ transfected cells, n=2-3 per point. **B** Representative blots from adPPARγ transfected cells.

Supplementary Fig. 5 Influence of direct PPARγ action on insulin sensitivity. **A** Effect of myocyte differentiation on PPARγ action induced insulin sensitization. C2C12 myocytes were studied at the indicated degrees of differentiation. Cells were treated as detailed in Figure 4A, and the resultant lysates blotted for pAKT. **B** PPARγ action rescues lipid-inhibited insulin signaling in FAT knockdown myotubes treated for 18 h with 0.75 mM palmitate and 0.3 mM albumin.

Supplementary Fig. 6 Influence of direct PPARγ action on insulin sensitivity. **A** Phosphotyrosine content of IRS-1 in C2C12 myotube lysates immunoprecipitated (IP) then immunoblotted (IB) with the indicated antibodies. The lack of effect of palmitate on insulin stimulated IRS-1 tyrosine phosphorylation recapitulates described results (Supplemental Reference 4). **B** PI3-kinase activity in IRS-1 immunoprecipitates from C2C12 myotubes receiving the indicated treatments. **C D** Phosphorylation of glycogen synthase kinase 3β (GSK3β) and glycogen synthase (GS) in C2C12 myotubes under the indicated conditions. N=3-4, *$p<0.05$ versus no insulin, # $p<0.05$ versus PPARγ/rosiglitazone treated cells. **E** Glycogen synthesis over 30 min in FAT knockdown (shFAT.1 middle panels and shFAT.3 right panels) and control (shGFP, left panels) myotubes treated with 0 (basal, bottom panels, white bars) or 100 nM insulin (bottom panels, black bars). Top panel shows the difference between the insulin-stimulated and basal states (grey bars) . n=3, *$p<0.05$ for change induced by insulin.

Supplementary Fig. 7 A Blood glucose (left panel) and glucose infusion rates (GIR, right panel) in mice infused with 6 mU/kg/min insulin; shown to document achievement of steady state during the final 40 minutes for the experiment shown in Figure 5F. **B** Extra-cellular acidification rates (ECAR) in C2C12 cells that had been exposed to 0.75 mM palmitate for 24 hours prior (red triangles) or not. Two groups received insulin (blue squares and red triangles) when indicated during the measurements. Cells received the indicated additions during the measurements. N=3. **C** mRNA expression in C2C12 myotubes. *$p<0.05$ versus PPARγ group, *** $p<0.0005$ versus adGFP transfected cells, ### $p<0.0005$ versus all other groups, n=3.

Supplementary Fig. 8 Influence of PPARγ action on lipotoxic myocellular lipid clearance and accumulation. **A** Clearance of palmitate-labeled myocellular lipids. Cells were labeled with 0.75 mM 0.5 μCi/mL [9,10-^{3}H]palmitate + 0.3 mM albumin over one day as described in Figure 6b. Cell lipid was extracted at 0 h (black lines), at which time [9,10-^{3}H]palmitate was replaced by unlabeled palmitate, and at 4 (blue lines) and 8 (red dotted lines) h thereafter. Radioactivity in the extracted lipids was separated by thin layer chromatography, identifying peaks corresponding to phosphatidylinositol (PI), phosphatidylcholine (PC), phosphatidylethanolamine (PE), unesterified palmitate (free), and triglycerides (TG). Myotubes were treated with adGFP and vehicle (top panel) or adPPARγ and 500 nM rosiglitazone (bottom panel); note the expanded y-axis scale in the lower panel. **B** DAPI (blue) and AdipoRed (green) staining of neutral lipid droplets in myotubes cultured with 0.75 mM palmitate + 0.3 mM albumin. **C** Ceramide in myotubes (n=6-8 per group), measured in the same cultures in which diacylglycerol was measured (Figure 6d).

Supplementary Table 1 Gene names, abbreviations, and NCBI Gene ID

Supplementary Table 2 PCR primers and conditions.

Supplementary Table 3 Effect of myocyte differentiation on PPARγ induced fatty acid uptake.

Supplemental Figure 1

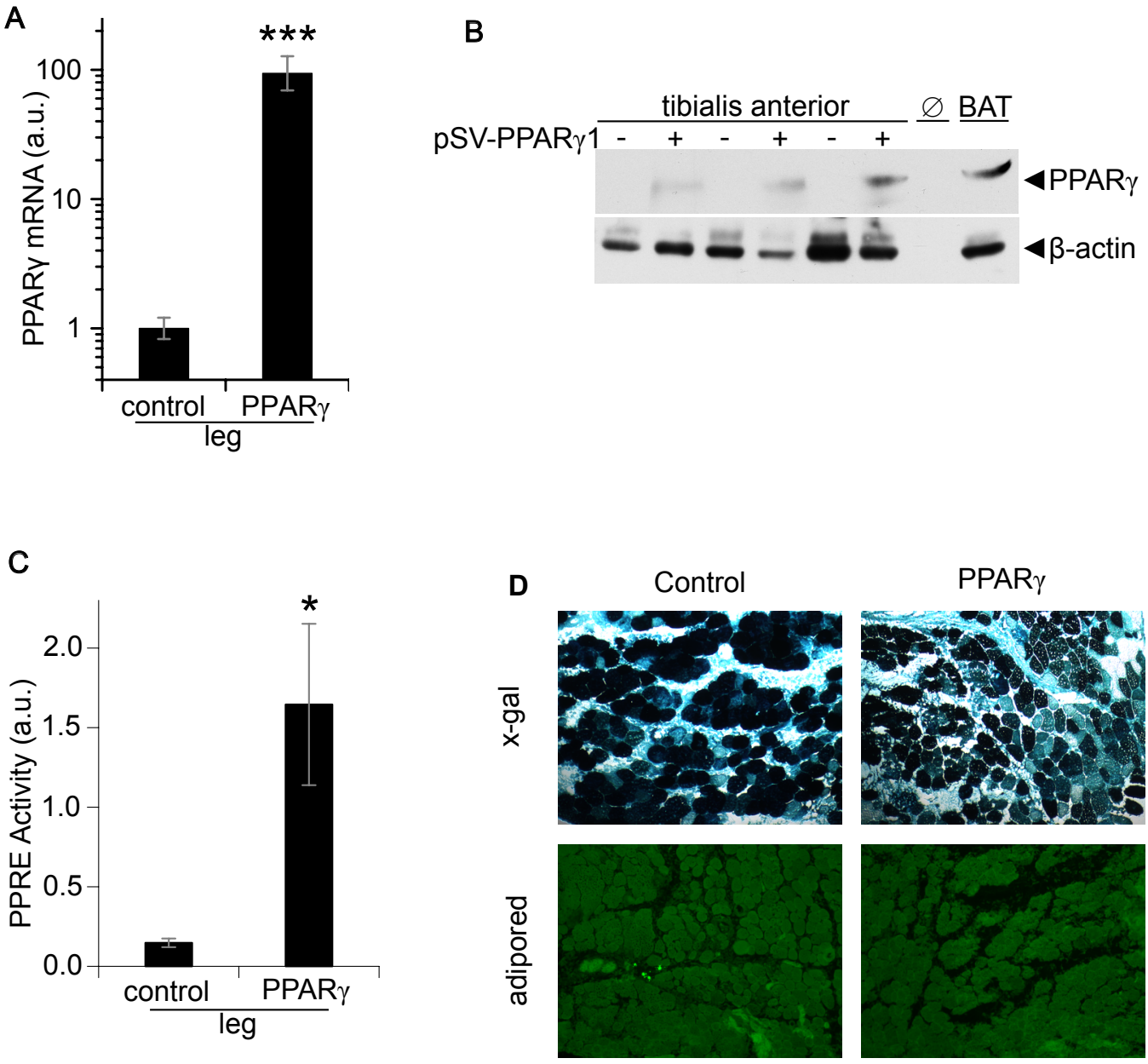

Supplemental Figure 2

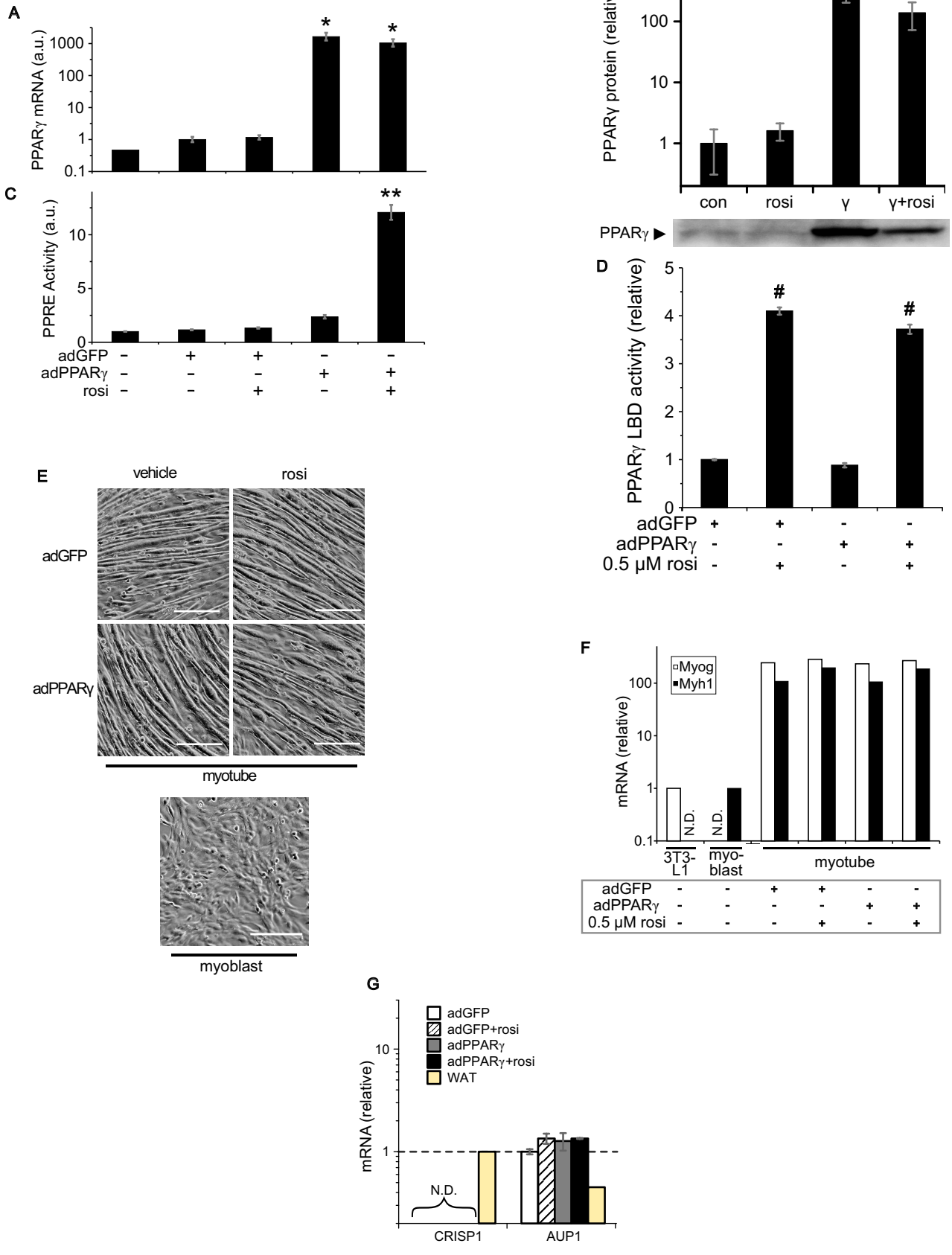

Supplemental Figure 3

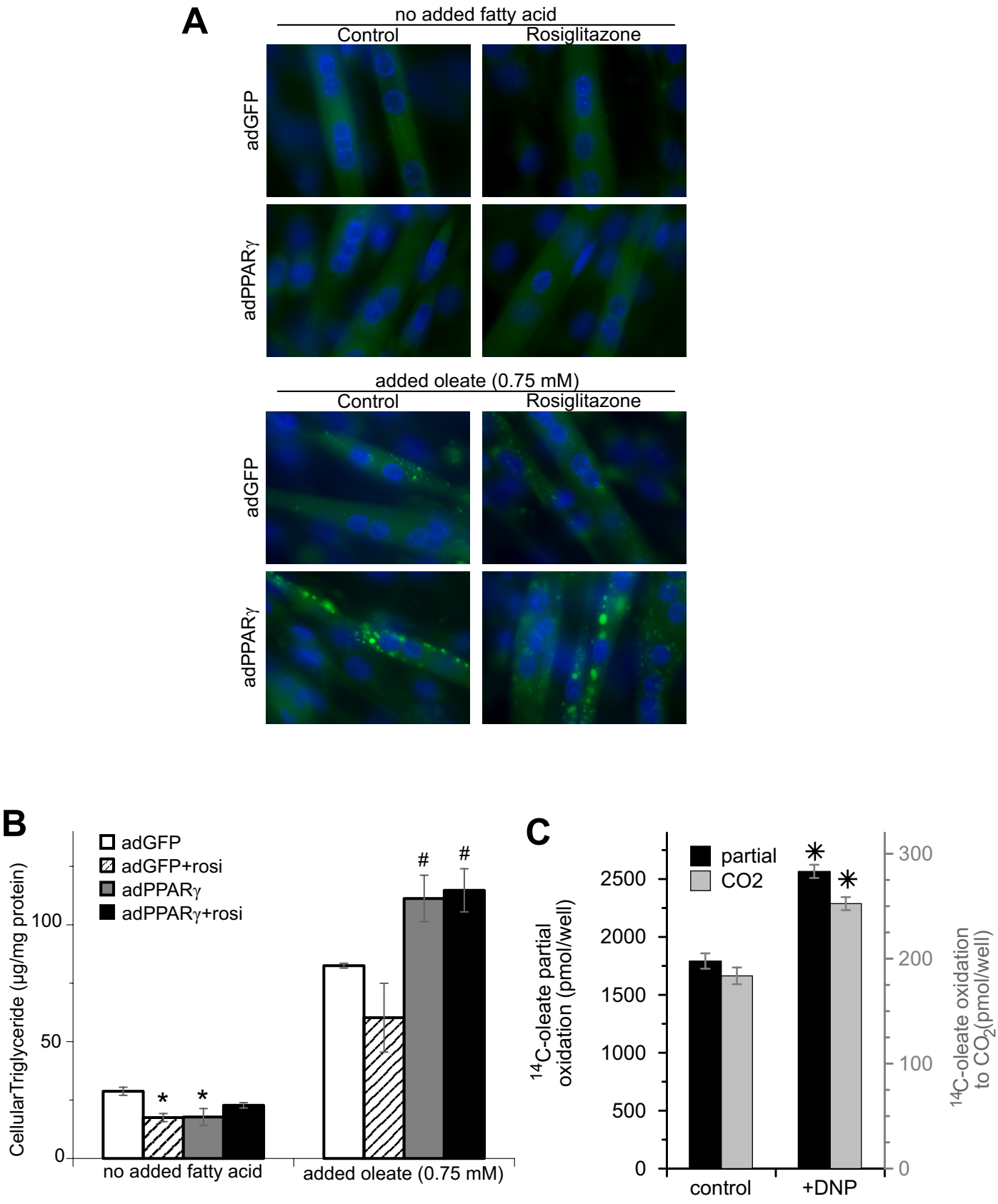

Supplemental Figure 4

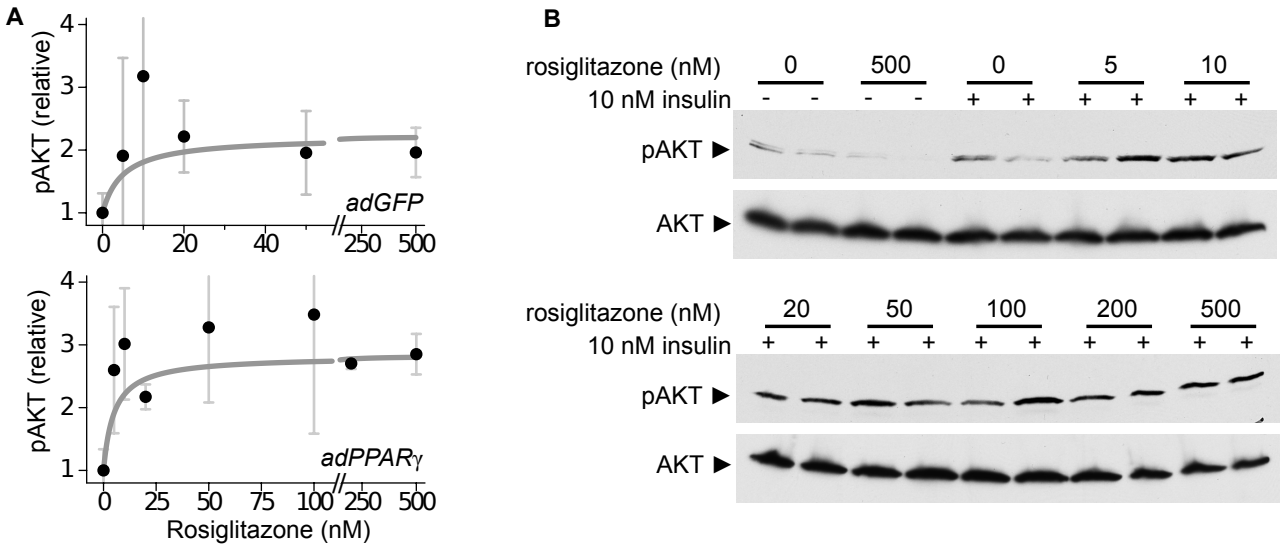

Supplemental Figure 5

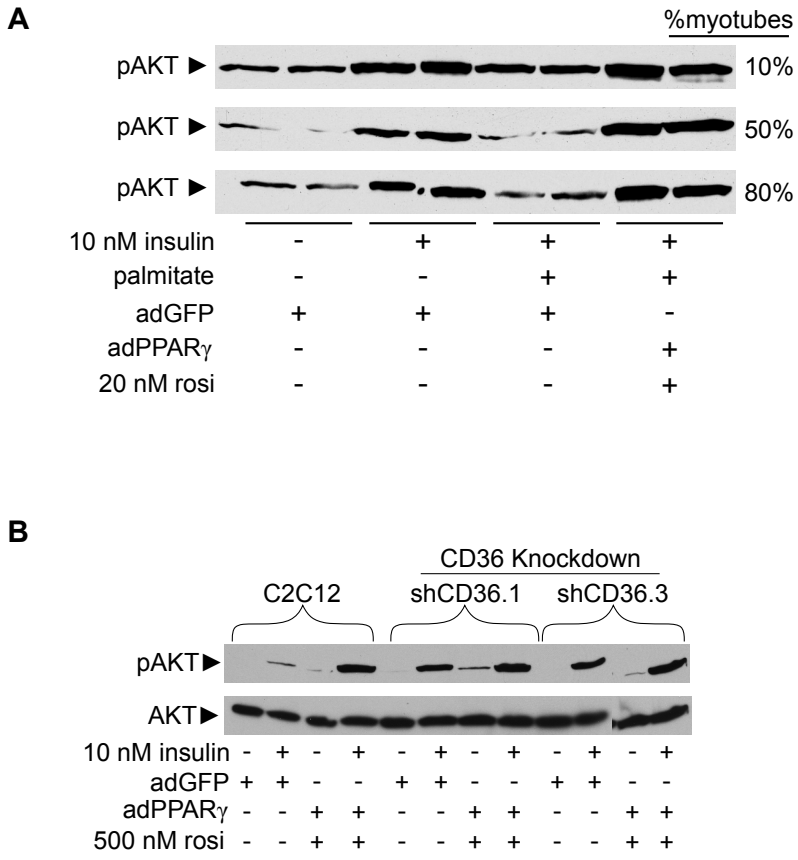

Supplemental Figure 6

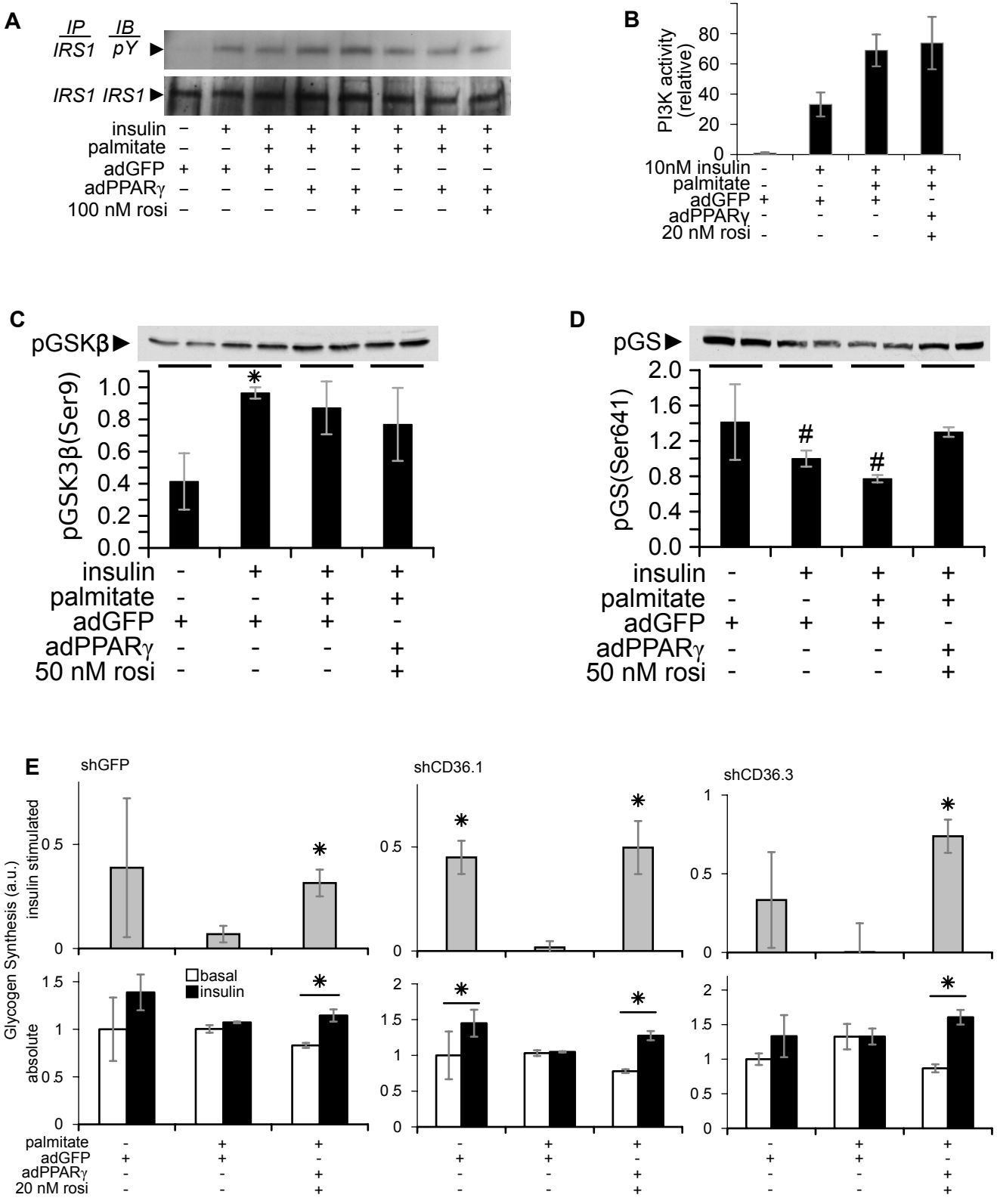

Supplemental Figure 7

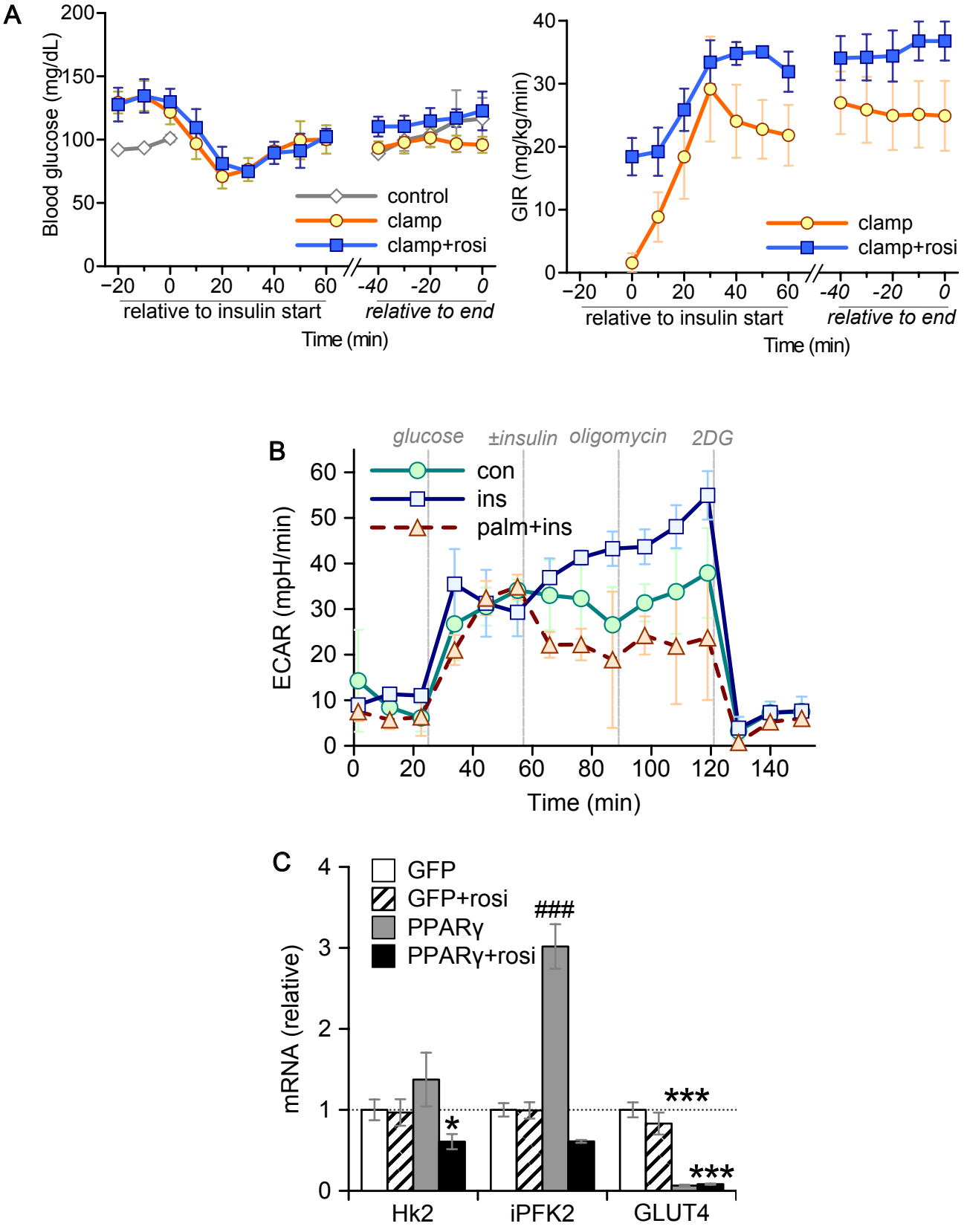

Supplemental Figure 8

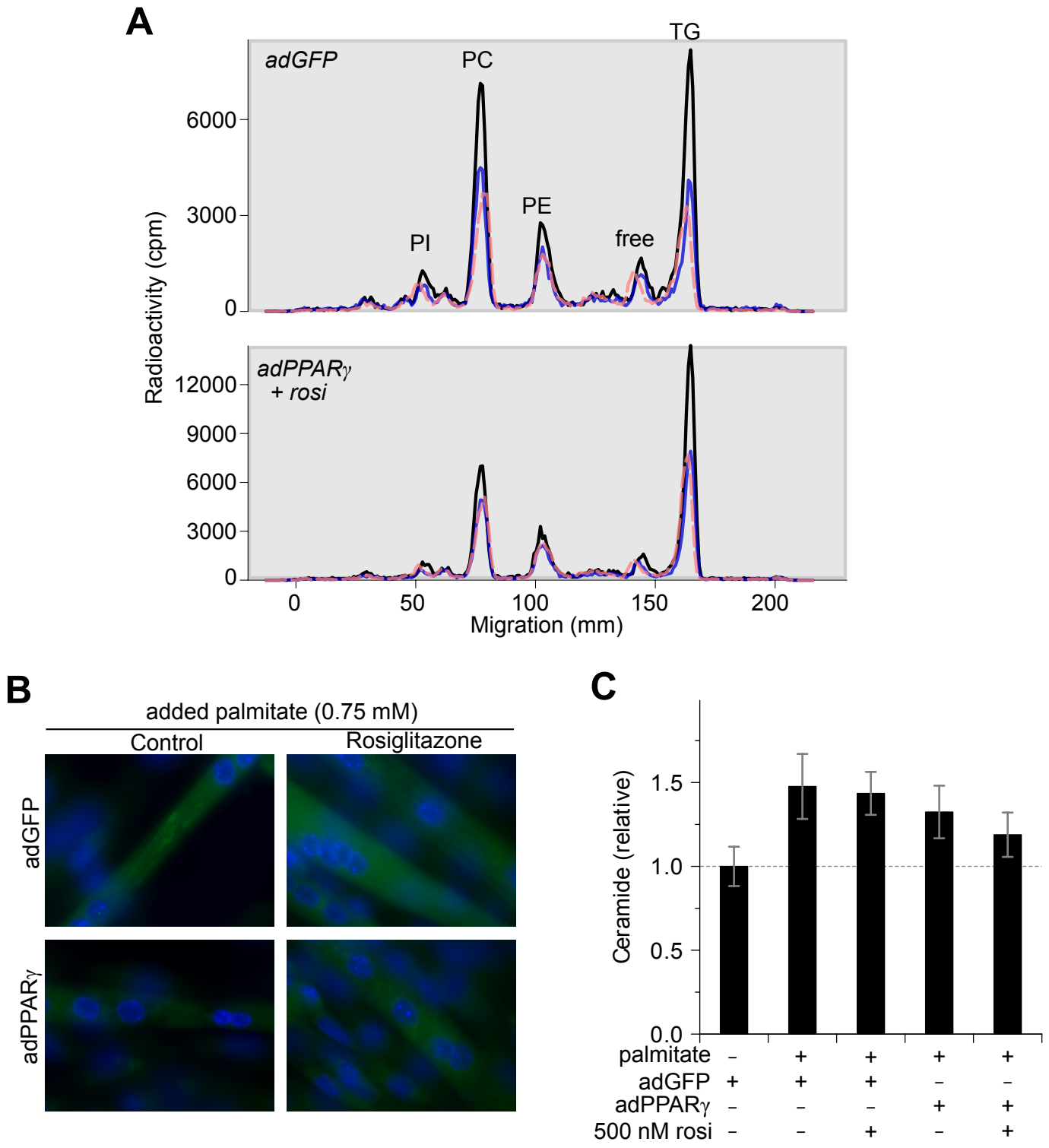

SUPPLEMENTAL TABLES

Supplemental Table 1:

manuscript		NCBI GENE	
abbrev.	**name**	**symbol**	**ID**
ACOX1	acyl-CoA oxidase	Acox1	11430
Actb	beta actin	Actb	11461
AKT	thymoma viral proto-oncogenes	-[a]	
AUP1	ancient ubiquitous protein 1	Aup1	11993
CPT1B	muscle-type carnitine palmitoyltransferase I	Cpt1b	12895
CRISP1	cysteine-rich secretory protein 1	Crisp1	11571
CD36	CD36	Cd36	12491
FABPpm	plasma membrane-associated fatty acid-binding protein	Got2	25721
FATP1	fatty acid transport protein 1	Slc27a1	26457
FATP4	fatty acid transport protein 1	Slc27a1	26569
GLUT4	glucose transporter type 4	Slc2a4	20528
GSK3β	glycogen synthase kinase 3 beta	Gsk3b	56637
GYS	glycogen synthase	-[a]	
GYS1	glycogen synthase 1, muscle	Gys1	14936
Hk2	hexokinase-2, muscle	Hk2	15277
iPFK2	6-phosphofructo-2-kinase	Pfkfb3	170768
IRS1	insulin receptor substrate 1	Irs1	16367
LCHAD	long chain hydroxyacyl-CoA dehydrogenase	Hadha	97212
MCAD	medium chain acyl-CoA dehydrogenase	Acadm	11364
Myh1	myosin heavy chain 1	Myh1	17879
Myog	Myogenin	Myog	17828
p85	phosphoinositide-3-kinase, p85 regulatory subunits	-[a]	
PDK1	3-phosphoinositide dependent protein kinase 1	Pdpk1	18607
PI3K	phosphoinositide-3-kinase complex	-[b]	
PKCθ	protein kinase C theta	Prkcq	18761
PPARγ	peroxisome proliferator activated receptor γ	Pparg	19016
PP2A-r2b	protein phosphatase 2A, regulatory subunit B beta	Ppp2r2b	72930
PP2A-r3a	protein phosphatase 2A, regulatory subunit B'' alpha	Ppp2r3a	235542
PYGM	muscle glycogen phosphorylase	Pygm	19309
Trib3	tribbles homolog 3	Trib3	246273

[a] - more than one isoform from separate genes

[b] - protein complex

Supplemental Table 2: PCR primers and conditions.

Gene	Protocol	Direction	Primer (5'-3')
Pparg	*a*	Forward	ATCAGGCTTCCACTATGGAGTT
		Reverse	TAAGCTTCAATCGGATGGTTCT
Cd36	*b*	Forward	CAATGGAAAGGATAACATAAGCA
		Reverse	GATCCGAACACAGCGTAGATAGA
Actb	*a,b*	Forward	GAGATTACTGCTCTGGCTCCT
		Reverse	GGACTCATCGTACTCCTGCTT
Myog	*a*	Forward	GGCAATGCACTGGAGTTCG
		Reverse	AGGCAACAGACATATCCTCCA
Myh1	*a*	Forward	TCGATGACCTCGCTAGTAACA
		Reverse	CCTTGGTCTTCAGCTCACTCA
Slc27a1	*b*	Forward	GGACGTGGCTGTGTATGG
		Reverse	GCAGAAGACGCAGGAAGA
Aup1	*b*	Forward	CTCTGTGACGGTGTCAGATGC
		Reverse	TGGGATGAAGCCACCTTACT
Cebpa	*b*	Forward	GTGGACAAGAACAGCAACGA
		Reverse	TCACTGGTCAACTCCAGCAC
Crisp	*b*	Forward	GTTGCATGTGGAGTTGCTGAAT
		Reverse	CTTCCTTGATAATTGCCAACAG
Got2	*b*	Forward	CAGATCGGCATGTTCTGTTTC
		Reverse	ACCGGATCTATTCACCACCAC
Slc27a4	*b*	Forward	GCAGATGTGGCAGTTTATGG
		Reverse	CAAGAAGCGCAGGAAGATG
Hadha	*C*	Forward	ACGCCTTGACCACAGGTTTCGG
		Reverse	TTGCGACCTAAGAAGCCCTTGGAG
Acox1	*C*	Forward	GCGCCGTCGAGAAATCGAGAAC
		Reverse	TCAGGGTCTGCGATGCCAAATTCC
Cpt1b	*C*	Forward	TTTGGTCCCGTGGCGGATGATG
		Reverse	TCCAACAGTGCTTGGCGGATGTG
Adadm	*C*	Forward	AACTAAACATGGGCCAGCGATGC
		Reverse	AGCTGCGACTGTAGGTCTGGTTC
Gys1	*C*	Forward	GCTGATGTGTTCCTGGAGGCATTGG
		Reverse	TTGGCTGTGTCCCATAGTTGTTTGC
Pygm	*C*	Forward	ACAAGCGGCAGCTCCTCAACTG
		Reverse	GGTGCAGCCTTGCCTCCAATC
HK2	*C*	Forward	CCTGGACCAGAGCATCCTCCTCAA
		Reverse	ATTTACCACGGCCACCACATCCA
Pfkfb3	*C*	Forward	TCGATGCTGGTGTGTGTGAGGAAC
		Reverse	AGGCGTTGGACAAGATCCTGGTAG
Slc2a4	*C*	Forward	ATGGCTGTCGCTGGTTTCTCCAA
		Reverse	AAGGACCCATAGCATCCGCAACA
Ppp2r2b	*C*	Forward	ATGGAATGGGTCAGACAGCGTCATC
		Reverse	TGGTGTTTCGGTCGAACATCCTGAAG
Ppp2r3a	*C*	Forward	ATACCCACCCTGGCCTCACCTTC
		Reverse	TCTGAACAACCGTGGTGATGTAGCG
Trib3	*C*	Forward	GCTCTTCCGGCAGATGGCTAGTG
		Reverse	ACCAGCTTCGTCCTCTCACAGTTG

Protocol a: 50°C for 30 min, 95°C for 5 min, 40 cycles of 95°C for 10 seconds and 55°C for 30 seconds.
Protocol b: 95°C for 10 min, 40 cycles of 95°C for 9 seconds, 60°C for 18 seconds and 72°C for 18 seconds.
Protocol c: 95°C for 10 min, 40 cycles of 95°C for 15 seconds, 60°C for 60 seconds.

Supplemental Table 3:

Effect of myocyte differentiation on PPARγ induced fatty acid uptake. C2C12 myocytes were studied at varying degrees of differentiation. Uptake of 80 μM oleate with 40 μM albumin was measured after a 30 minute incubation in cells having received the indicated treatments. N=3 for all groups.

	myotube content		
group	10%	50%	80%
	relative oleate uptake (%)		
adGFP	100±11	100±2	100±1
adGFP+rosi	93±1	91±1	94±7
adPPARγ	74±6[a]	100±7	112±4
adPPARγ+rosi	63±1[a,b]	109±1	124±7[b]

[a] $p<0.05$ versus adGFP

[b] $p<0.05$ versus adGFP + rosi

Supplementary Methods

PPARγ Ligand Detection Plasmids pFA-CMV and pFR-SEAP were from Stratagene (La Jolla, CA). pFA-PPARγ-LBD was created by ligating the cDNA encoding the ligand binding domain (Cys163 - Tyr475) of PPARγ1 into pFA-CMV. Media from myotubes transfected with pFA-PPARγ-LBD and pFR-SEAP were assayed using with CSPD® Substrate (Applied Biosystems; Foster City, CA).

Identification of Adipocyte-Selective Expression Markers Transcripts of interest were identified from public microarray datasets: Diabetes Genome Anatomy Project (http://www.diabetesgenome.org/) samples jos2250,2347,2433 and jos2456,2470,2471 representing skeletal muscle and white adipose tissue from 6 week old C57Bl/6 mice respectively; Gene Expression Omnibus (www.ncbi.nlm.nih.gov/geo/) dataset GDS734 samples GSM24459,60,61 and GSM24464,65,66 representing mature 3T3-L1 adipocytes under control conditions or treated for 1 day with 1 μM rosiglitazone. AUP1 was the transcript most highly regulated by thiazolidinediones in mature adipocytes, as determined by absolute t-statistic, among genes with adipose expression in the top quartile and with the difference in muscle and adipose tissue expression in the lowest quartile. CRISP1 exhibited the highest absolute increase in expression between adipose tissue and muscle among genes with the lowest quartile of thiazolidinedione responsiveness and highest quartile of adipose expression.

Supplementary References

1. **Hu E, Tontonoz P, Spiegelman BM** 1995 Transdifferentiation of myoblasts by the adipogenic transcription factors ppar gamma and c/ebp alpha.. Proc Natl Acad Sci U S A 92:9856-9860
2. **Kausch C, Krützfeldt J, Witke A, Rettig A, Bachmann O, Rett K, Matthaei S, Machicao F, Häring HU, Stumvoll M** 2001 Effects of troglitazone on cellular differentiation, insulin signaling, and glucose metabolism in cultured human skeletal muscle cells.. Biochem Biophys Res Commun 280:664-674
3. **Singh J, Verma NK, Kansagra SM, Kate BN, Dey CS** 2007 Altered ppargamma expression inhibits myogenic differentiation in c2c12 skeletal muscle cells.. Mol Cell Biochem 294:163-171
4. **Schmitz-Peiffer C, Craig DL, Biden TJ** 1999 Ceramide generation is sufficient to account for the inhibition of the insulin-stimulated pkb pathway in c2c12 skeletal muscle cells pretreated with palmitate.. J Biol Chem 274:24202-24210